Hindawi Publishing Corporation
International Journal of Polymer Science
Volume 2014, Article ID 374368, 11 pages
http://dx.doi.org/10.1155/2014/374368

Review Article

Poly(3-hydroxybutyrate) and Poly(3-hydroxybutyrate-co-3-hydroxyvalerate): Structure, Property, and Fiber

Qingsheng Liu,[1] Hongxia Zhang,[2] Bingyao Deng,[1] and Xiaoyan Zhao[3]

[1] *Key Laboratory of Eco-Textiles (Ministry of Education), Jiangnan University, Wuxi 214122, China*
[2] *Wuxi Entry-Exit Inspection and Quarantine Bureau, Wuxi 214101, China*
[3] *School of Petrochemical Engineering, Changzhou University, Changzhou 213164, China*

Correspondence should be addressed to Qingsheng Liu; qsliu@jiangnan.edu.cn and Bingyao Deng; bydeng@jiangnan.edu.cn

Received 29 December 2013; Revised 19 March 2014; Accepted 17 April 2014; Published 13 May 2014

Academic Editor: Robert A. Shanks

Poly(3-hydroxybutyrate) [P(3HB)] and poly(3-hydroxybutyrate-co-3-hydroxyvalerate) [P(3HB-co-3HV)] are produced by various microorganisms as an intracellular carbon and energy reserve from agricultural feedstocks such as sugars and plant oils under unbalanced growth conditions. P(3HB) and P(3HB-co-3HV) have attracted the attention of academia and industry because of its biodegradability, biocompatibility, thermoplasticity, and plastic-like properties. This review first introduced the isodimorphism, spherulites, and molecular interaction of P(3HB) and P(3HB-co-3HV). In addition, the effects of 3HV content on the melting temperature and crystallization rate were discussed. Then the drawbacks of P(3HB) and P(3HB-co-3HV) including brittleness, narrow melt processing window, low crystallization rate, slow biodegradation rate in body, and so on were summarized. At last, the preparation, structure, and properties of P(3HB) and P(3HB-co-3HV) fiber were introduced.

1. Introduction

Polyhydroxyalkanoates (PHAs) are a kind of biodegradable and biocompatible polyesters produced by various microorganisms as an intracellular carbon and energy reserve from agricultural feedstocks such as sugars and plant oils under unbalanced growth conditions [1, 2]. The ideal life cycle of microbially-produced PHAs is a closed-loop process. Plants such as corn, sugarbeet, or wheat use the sun's energy to convert water and carbon dioxide in the atmosphere into sugar inside the plant tissue via photosynthesis. These plants are subsequently processed to yield sugar that serves as the feed to a microbial fermentation process, in which microbes accumulate polymer as intracellular granules. Once the cells are harvested, the polymer is extracted, concentrated, and dried. It can then be processed to make useful products by different methods including injection molding, blow molding, melt spinning, and so on. Under normal conditions, these products are stable. However, when placed in a microbially-active environment such as a compost heap, which has high temperature and high humidity, they will biodegrade. Ideally, this process occurs aerobically, yielding water and carbon dioxide in the same proportions that were originally used in the photosynthesis [3, 4].

Poly(3-hydroxybutyrate) [P(3HB)] and poly(3-hydroxybutyrateco-3-hydroxyvalerate) [P(3HB-co-3HV)] are the most studied polyesters in the PHA family [5]. The chemical structures of P(3HB) and P(3HB-co-3HV) were shown in Figure 1. The biodegradability behavior of P(3HB) and P(3HB-co-3HV) depended on the composition of the polymer, the environment conditions, and specimen shape [6–11]. P(3HB) biodegraded at a rate of 3.6 wt% per week in activated sludge, 1.9 wt% per week in soil, 1.5 wt% per week in lake water, and 0.8 wt% per week in Indian Ocean sea water [10]. The degradation rates for P(3HB-co-40 mol% 3HV) were 17.8 wt% per week in activated sludge, 6.7 wt% per week in

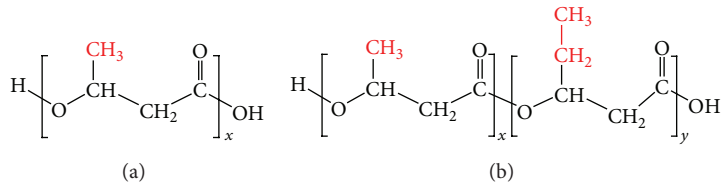

Figure 1: Chemical structure of P(3HB) (a) and P(3HB-co-3HV) (b).

soil, 3.2 wt% per week in lake water, and 2.7 wt% per week in Indian Ocean sea water [10]. Weng et al. [11] studied the biodegradation behavior of P(3HB-co-3HV) with different HV content under controlled aerobic composting conditions according to ISO 14855-1. The order of biodegradability was P(3HB-co-40 mol% 3HV)> P (3HB-co-20 mol% 3HV)> P (3HB-co-3 mol% 3HV)> P (3HB). Li et al. [12] found that P(3HB-co-3HV) degraded faster than P(3HB) in a medium with PHA depolymerase. However, Boyandin et al. [13] studied microbial degradation of polyhydroxyalkanoates in tropical conditions by microbial communities of Vietnamese soils in locations close to Hanoi and Nha Trang. The results showed that P(3HB) was degraded at higher rates than P(3HB-co-3HV). In addition, they found that the average rates of mass loss were 0.04–0.33% per day for films and 0.02–0.18% for compact pellets. PHA degradation was accompanied by a decrease in the polymer molecular mass and, usually, an increase in the degree of crystallinity. The biocompatibility of P(3HB) and P(3HB-co-3HV) has been studied by a large number of research groups and has been found to have low toxicity, in part due to the fact that it degrades in vivo to D-3-hydroxybutyrate, a normal constituent of human blood [14–16].

Moreover, the P(3HB) and P(3HB-co-3HV) polymers, being saturated polyesters, behave similarly to conventional petroleum derived thermoplastics such as polypropylene (PP) and polyethylene (PET) [5]. In addition, P(3HB) and P(3HB-co-3HV) are thermoplastic, which can be melt processed into a wide variety of consumer products including plastics, films, and fibers [17]. Because of thermoplastics, renewability, biodegradability, good biocompatibility, and mechanical properties similar to PP and PET, P(3HB) and P(3HB-co-3HV) have recently attracted much public and industrial interest as substitute of the fossils fuels. They have been evaluated for a variety of applications, which include environmentally friendly materials and biomedical materials for controlled release, surgical sutures, wound dressings, lubricating powders, tissue engineering, and so on [18, 19].

Up to now, there are a number of reviews on P(3HB) and P(3HB-co-3HV). These reviews cover biosynthesis [20–32], biodegradation [32–35], chemomechanical properties [36], blends [37–39], and application [40–45]. However, some new results were reported on crystallization behavior and crystalline structure. In addition, few reviews on drawbacks and fiber of P(3HB) and P(3HB-co-3HV) have been done. Therefore, in this review, literatures on drawbacks and fiber of P(3HB) and P(3HB-co-3HV) and some new results on crystallization behavior and crystalline structure of P(3HB) and P(3HB-co-3HV) will be reviewed.

2. Crystallization Behavior and Crystalline Structure

2.1. Isodimorphism. The most common crystal structure of the P(3HB) and P(3HB-co-3HV) is the *a*-form, which is produced under the typical conditions of melt, cold, or solution crystallization [36]. The unit cells belong to orthorhombic, $P2_12_12_1$ (D_2^4) ($\alpha = \beta = \gamma = 90^\circ$) with $a = 0.576$ nm, $b = 1.320$ nm, and $c = 0.596$ nm (fiber repeat) for P(3HB) and $a = 0.952$ nm, $b = 1.008$ nm, and $c = 0.556$ nm (fiber repeat) for P(3HV) [46]. P(3HB-co-3HV) crystallizes either in a P(3HB) or P(3HV) crystal lattice. The monomer units of one type are partially included in the crystal lattice of the other and vice versa [46–49]. Kunioka et al. [46] reported that P(3HB-co-3HV) from 0 to 37 mol% crystallized in the P(3HB) lattice, while those with the 3HV composition from 53 to 95 mol% crystallized in the P(3HV) lattice. The transformation from the P(3HB) lattice to the P(3HV) lattice occurred at approximately 40 mol% 3HV. This phenomenon was called isodimorphism. Bloembergen et al. [48] reported that the transformation happened at about 30 mol% 3HV. Scandola et al. [47] found that the value was 41 mol%. In the copolymer containing 41 mol% 3HV units, P(3HB)- and P(3HV)-type crystals coexisted. The composition of this copolyester corresponded to the so-called pseudoeutectic, where the crystalline phase of an isodimorphic system changed from the characteristic of one homopolymer to that of the other. It was expected that the two crystals were found side by side close to the pseudoeutectic.

Kunioka et al. [46] measured *d* spacings of the (110), (020), and (002) plane of P(3HB) and P(3HB-co-3HV). The (110) *d* spacing apparently increased as the 3HV content increased to 37 mol% because the ethyl side chains of 3HV units expanded the (110) plane of the P(3HB) lattice. The (020) and (002) *d* spacings remained unchanged. Therefore, only the *a* parameter of the unit cell changed. Similar results were obtained by Bluhm et al. [49]. For P(3HB-co-3HV) with 3HV = 53~95 mol%, all *d* spacings were invariant in the P(3HV) lattice [46]. However, Scandola et al. [47] found that in the P(3HB)-type phase, both *a* and *b* unit cell dimensions underwent a moderate but gradual increase with increasing 3HV content. In regards to the copolymers crystallizing in the P(3HV) lattice, it was found that replacement of 3HV with 3HB units induced a decrease of the *b* parameter, in agreement with the smaller steric hindrance of the methyl side chain. The expansion of the P(3HB) lattice on increasing 3HV content was larger than contraction of the P(3HV) unit cell on introduction of 3HB units. In addition, Barker et al. [50] found that the amount of cocrystallization of 3HV in

the P(3HB) crystal structure decreased with the increase of the crystallization temperature. Yoshie et al. [51] found a structural transition at ca. 10 mol% HV in P(3HB-co-3HV). The composition dependence of spherulite growth rate, crystallinity, lamella thickness, 3HV content in the crystalline phase, and the melting temperature changed discontinuously at ca. 10 mol% HV [51].

For P(3HB-co-3HV), the crystallinity degree (X_c) decreased when the relative fraction of foreign monomer units becomes larger. The P(3HB) lattice, where the crystalline fraction changed from 73% [P(3HB)] to 52% [P(3HB-co-34 mol% 3HV)] was more sensitive to commoner inclusion than the P(3HV)-type phase, where X_c = 68% and 60% for P(3HB-co-95 mol% 3HV) and P(3HB-co-55 mol% 3HV), respectively [47]. Although X_c of P(3HB-co-3HV) changed with composition, P(3HB-co-3HV) owned high X_c (>50%) when 3HV content changed from 0 to 95 mol% because of isodimorphism [51]. The melting temperature (T_m) of P(3HB-co-3HV) had its minimum value at the transformation composition. T_ms of P(3HB-co-3HV) with different 3HV content are listed in Table 1 [52].

For P(3HB-co-3HV), the crystallization rate strongly depended on copolymer composition. When 3HV content was below the composition where the crystalline phase changed from the P(3HB) to the P(3HV) lattice, the crystallization process markedly slowed down with the increase of 3HV content. When 3HV content was above the composition where the crystalline phase changed from the P(3HB) to the P(3HV) lattice, the crystallization rate of P(3HB-co-3HV) increased with the increase of 3HV content [47]. The crystallization rate depends on both rates of nucleation and crystal growth. In the P(3HB-co-3HV) sample that crystallized in the P(3HV) lattice, the ethyl side chains of 3HV units prevented crystallization of P(3HB) lattice due to the steric effects. Both the rates of nucleation and crystal growth were much slower than those of P(3HB) homopolymer [46]. In contrast, both the rates of nucleation and crystal growth were not affected by the methyl side chains of 3HB units in the P(3HB-co-3HV) sample that crystallized in the P(3HV) lattice [46]. The crystallization rate decreased in the following series: P(3HB) ≈ *P*(3HB-co-83 mol% 3HV) ≫ *P*(3HB-co-21 mol%3HV) [46].

In addition, it is worth noting that another kind of crystal exists in P(3HB) and P(3HB-co-3HV), called β-form crystal. The β-form crystal is a strain-induced paracrystalline structure of highly extended chains corresponding to a twisted planar zigzag conformation, which has been reviewed by Laycock et al. [36].

2.2. Spherulitic Morphology. For P(3HB) and P(3HB-co-3HV), nonbanded spherulites or banded spherulites could be formed, which was determined by crystallization conditions. Ding and Liu [53] observed the spherulites morphologies of P(3HB) crystallized isothermally from thin melt film with different crystallization temperatures. It was found that the nonbanded spherulites could be observed at lower and higher crystallization temperatures, and the banded spherulites were formed usually at an intermediate range. With the increase of crystallization temperature, band spacing increased gradually. When the crystallization temperature was above $T_c^{\max}$ ($T_c^{\max}$, at which the copolyester exhibited the maximum spherulite radial growth rate), the band spacing increased rather markedly with crystallization temperature [47]. Jiang et al. [54] found that the surface of the banded spherulites of P(3HB-co-3HV) consisted of concentric ridges and valleys by tapping-mode AFM. The ridge surfaces in AFM images corresponded to the bright rings in the POM images. At the ridges, the lamellae were aligned in the edge-on orientation. At the valleys, the lamellae were arranged in the flat-on orientation and the surface was covered by a very thin layer of loose loops and protruding cilia. It was reported by Ding and Liu [53] that the change of the ratio of the crystallization rate (ν_c) and the diffusion (ν_d) would result in the transition of the spherulitic morphologies. The actual morphology and structure of the spherulites depended on the ratio between diffusive displacement of chains and crystallization rate. This ratio, in turn, could be controlled by a suitable choice of the crystallization temperature and thin film thickness for polymer thin film crystallization. For P(3HB) crystallization from thin melt film, three relationships of ν_c and ν_d could be considered, which were schematically drawn in Figure 2. Firstly, when the crystallization temperature was low or high, the value of ν_c was more than that of ν_d. The nonbanded spherulites were commonly formed. Secondly, when the crystallization temperature was an intermediate range, the value of ν_c was less than that of ν_d. The banded spherulites with ridge and valley structures formed periodically on the spherulitic surface are commonly formed. The third was $\nu_c = \nu_d$, which was located at the intersections of diffusion displacement and chain crystallization curves. There were two intersections located at lower and higher temperatures. When P(3HB) crystallized near the higher temperature intersection, the banded spherulite was still formed but the banding was distorted to highly zigzag irregularity. At the vicinity of the lower temperature intersection, the spherulitic morphology was also distorted banding but the band spacing was too small to observe. Ding and Liu [53] thought that the banded spherulites formed in the thin films might mainly come from lamellar twist and rhythmic crystal growth. The overall growth rates at ridges and valleys which appeared periodically on the surface of the spherulite were different obviously. The band spacing was proportional to the diffusion length of melt molecules and increased with an increase in crystallization temperature. With further increase of crystallization temperature, the ring band was mainly caused by the lamellar twist. Wang et al. [55] investigate the link between

Table 1: The relationship between melting temperature (T_m) of P(3HB-co-3HV) and the content of 3HV [52].

3HV (mol%)	T_m (°C)	3HV (mol%)	T_m (°C)
0	164/173	58.4	75/86
9	153/169	73.9	85
15	151/161	88.6	92
21	159	100	118
28.8	100	—	—

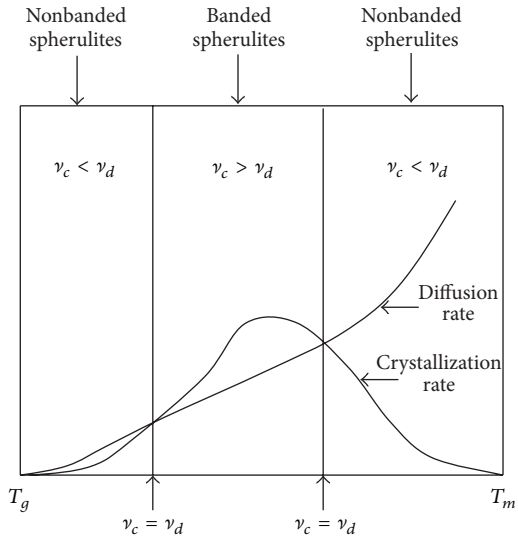

Figure 2: The transition of spherulitic morphology with change of the relationship of crystallization rate (ν_c) and diffusion rate (ν_d) [53].

configurational chirality and twist sense of lamellar crystals. The twist senses of P(3HB-co-3HV) lamellae with 0 mol% [P(3HB)] and 8 mol% 3HV were left-handed, but the ones of P(3HB-co-3HV) with 12 and 40 mol% 3HV were right-handed, which were the same as that of P(3HV). P(3HB-co-3HV), only increasing 3HV amount from 8 to 12 mol %, reverses the twist sense.

In addition, Liu et al. [56, 57] observed special spherulitic morphologies in two kinds of double crystalline block copolymers based on P(3HB-co-3HV), including P(3HB-co-3HV)-*b*-PEG [named PHEG*x*, in which *x* stood for the number-average molecular weight (M_n) of the corresponding reagent PEGs] and P(3HB-co-3HV)-*b*-PCL (named PHCL-y, in which y stood for the weight percent of PCL units). The banded structure also could be observed in PHEG1000. However, the banding spacing in PHEG1000 spherulites was narrower than the one in P(3HB-co-3HV), which was shown in Figure 3. In PHEG1000 banded spherulites, PEG1000 (PEG with M_n of 1000) was melt. The spherulite template and concentric spherulites could be observed in PHEGs and PHCLs because of the crystallization competition between one crystalline block and the other crystalline block, which was shown in Figure 4. In Figures 4(a)~4(c), the first grown spherulite acted as a template for the spherulite growth of the other block. When PHEG4000 crystallized isothermally at 36°C, the concentric spherulites could be observed (Figure 4(d)). The formation process of PHEG4000 concentric spherulite was shown in Figure 5.

2.3. Molecular Interaction. In the crystal structure of P(3HB), the distance between the O atom of the C=O group and the H atom of the CH_3 group was 2.63 Å, which was shorter than the van der Waals separation (2.72°) [58, 59]. The CH_3 asymmetric stretching band of P(3HB) appeared at an unusually high frequency (~3007 cm^{-1}) [59–61]. This indicated that the inter- or intra-C-H$\cdots$O=C hydrogen bonding between the CH_3 group of one helix and the O=C group of another helix in P(3HB) existed.

Sato et al. [52] also studied the weak molecular interaction of P(3HB-co-3HV) copolymers. The results showed that P(3HB-co-3HV) copolymers with low HV content have $CH_3\cdots$O=C hydrogen bonds in P(3HB) lattice, whereas P(3HB-co-3HV) with high 3HV content has $CH_2\cdots$O=C hydrogen bonds in P(3HV) lattice. When 3HV content of P(3HB-co-3HV) corresponds to the region of transition of the crystal structure from the P(3HB) type to the P(3HV) type, there are only weak intermolecular interactions between a C=O group and either a CH_2 group or a CH_3 group. The CH$\cdots$O=C hydrogen bonding stabilizes the chain folding in the structure of P(3HB) and P(3HB-co-3HV), and the high crystallinity of P(3HB) and P(3HB-co-3HV) partly comes from the CH$\cdots$O=C hydrogen bonding.

3. Drawbacks

The 3HV content of commercial P(3HB-co-3HV) is below 20 mol%. It can be seen from Table 1 [52] that the melting temperature of commercial P(3HB-co-3HV) was beyond 150°C. In addition, P(3HB) and P(3HB-co-3HV) were unstable above 160°C mainly by nonradical, random chain scission (*cis*-elimination) reaction, which resulted in a drastic reduction in molecular weight during melt processing. Therefore, the melt processing window of P(3HB) and P(3HB-co-3HV) was narrow [2, 62].

P(3HB) and P(3HB-co-3HV) are brittle materials, which makes them unsuitable for some applications. The probable causes are as follows [1, 63–67]. Firstly, bacterially synthesized P(3HB) and P(3HB-co-3HV) are completely isotactic stereoregular polyesters; they have a high tendency to crystallize. Secondly, the secondary crystallization will happen during storage at ambient temperature due to low glass transition temperature (T_g) (~5°C) of P(3HB) and P(3HB-co-3HV). Thirdly, the nucleation density of P(3HB) and P(3HB-co-3HV) is low because of high purity, which results in the formation of extremely large-size spherulites. The large-size spherulites and the secondary crystallization lead to interspherulitic cracking during storage of the polymer at room temperature, which is commonly known to impair the mechanical properties of the materials.

The crystallization rate of P(3HB) and P(3HB-co-3HV) is low because of low nucleation density. Bloembergen et al. [48] found that a melt-quenched P(3HB-co-3HV) sample containing 20 mol% HV was still amorphous after 15 min. Hu et al. [61] studied the isothermal melt-crystallization behavior of P(3HB-co-3HV) at 125°C. The results showed that the half-time for the crystallization, $t_{1/2}$, was 60 min or so. The low crystallization rate of P(3HB) and P(3HB-co-3HV) would make their films or fibers stick to themselves during melt processing.

In addition, P(3HB-co-3HV) does not readily degrade in the body because of its high crystallinity and hydrophobicity; thus it is unsuitable for short-term drug carriers, tissue-engineering scaffolds, and so on [68, 69].

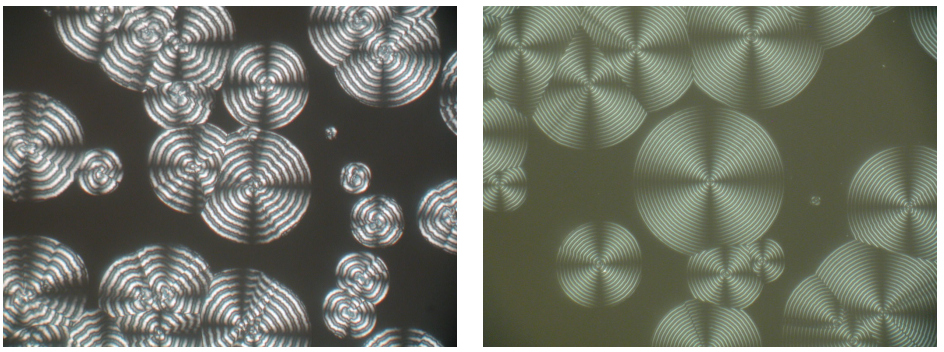

(a) (b)

Figure 3: POM photographs of PHBV2000 (a) and PHEG1000 (b) spherulites observed under isothermal crystallization at 25°C (in which PHBV2000 stood for the P(3HB-co-3HV) with the M_n of 2000) [56].

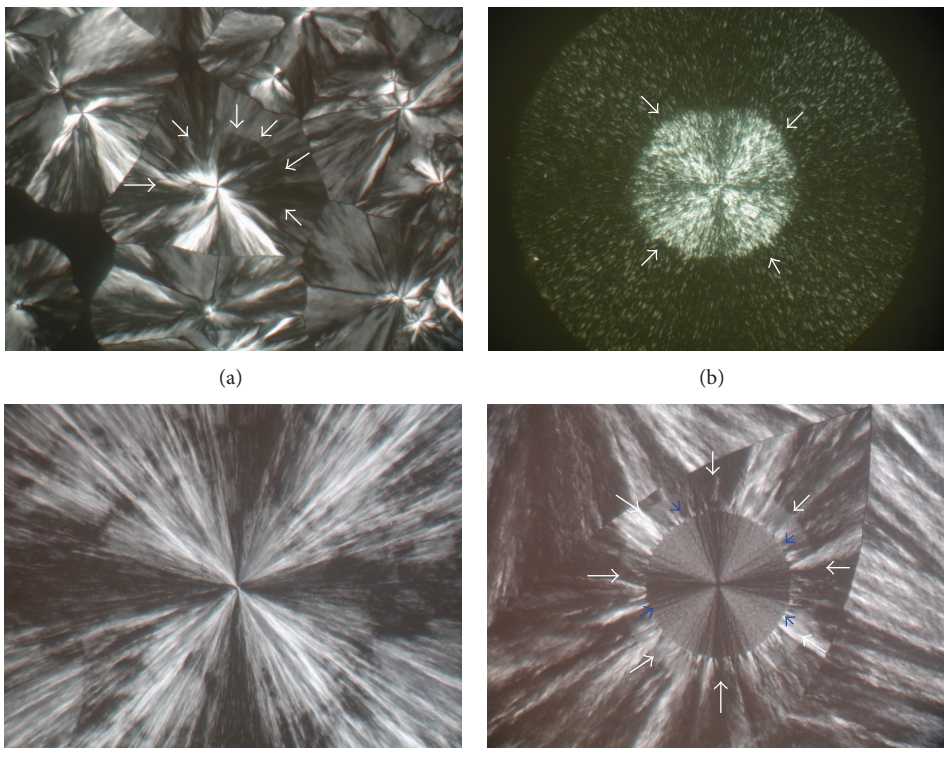

(a) (b)

(c) (d)

Figure 4: POM photographs of double crystalline block copolymers based on PHBV at different isothermal melt-crystallization temperatures. (a) PHCL-60, 30°C; (b) PHCL-60, 38°C; (c) PHEG4000, 30°C; and (d) PHEG4000, 36°C [56, 57].

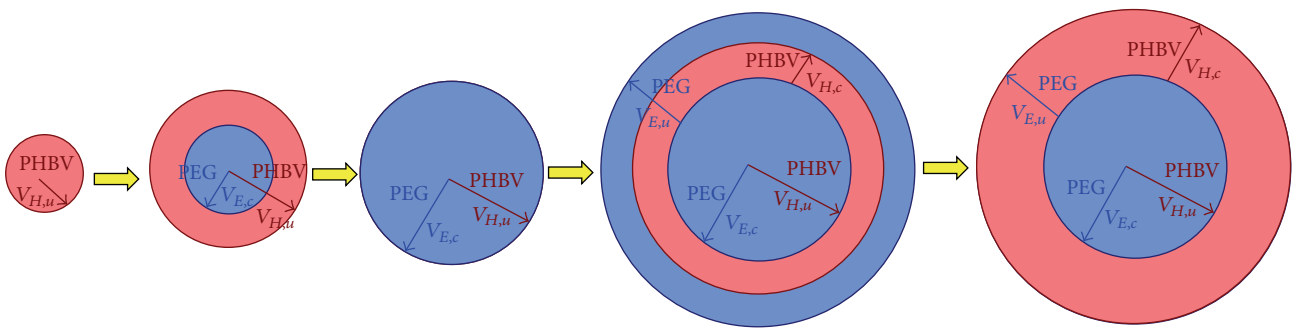

Figure 5: Schematic of formation process of PHEG4000 concentric spherulite at 36°C [56].

4. P(3HB) and P(3HB-co-3HV) Fiber

Only a few groups studied the preparation, structure, and properties of P(3HB) and P(3HB-co-3HV) fibers. Gordeyev et al. [70] obtained as-spun P(3HB) fibers with preorientation by melt spinning and drawing as quickly as possible while still hot. The preorientated as-spun P(3HB) fibers could be drawn to high draw ratios (DR) even after several weeks of storage at room temperature. In addition, they prepared the annealed P(3HB) fiber by following procedures. At first, the preorientated as-spun P(3HB) fibers were drawn to a total DR of about 8 at 110°C. Then the drawn sample, extended to 80% of its initial length at room temperature, was annealed at 155°C for 1 h to obtain the annealed fiber. The tensile strength and Young's modulus of the annealed fiber were 190 MPa and 5.6 GPa, respectively. Moreover, they [71] prepared P(3HB) fiber by gel spinning process. The processing temperature in the gel-spinning process was lower than the one in the melt spinning process, which could reduce the thermal degradation of P(3HB). Tensile strength, static modulus, and strain at break of the P(3HB) fiber prepared by gel spinning could reach 360 MPa, 5.6 GPa, and 37%, respectively.

Schmack et al. [72] prepared P(3HB) fibers by high-speed melt spinning and drawing, respectively. They found that the textile physical properties (elongation at break, tensile strength, and Young's modulus) depended on the spinning speed and the DR. When the DR was low, the fibers were brittle and had no significant elongation at break and tensile strength. When the DR was high, the fibers owned high tenacity, high modulus, and an acceptable elongation at break. The maximum tensile strength, the modulus, and elongation at break in the drawn fibers were about 330 MPa, 7.7 GPa, and 37%, respectively. When the drawn fibers with high DR were conditioned at room temperature for 3 days and 3 months, neither embrittlement of the fibers nor deterioration of the fiber properties due to the secondary crystallization took place to a large extent. The reasons were as follows. The fibers spun at high speeds and high DRs possessed orthorhombic (α modification) and hexagonal (β modification) crystals. The latter was attributed to stress-induced crystallization. The fiber structures formed during these processes were fibril-like, which resulted in the good mechanical properties. The fibers obtained by a low DR had spherulitic structures, which led to poor textile physical properties.

Yamane et al. [73] prepared P(3HB) fibers using P(3HB) containing some contaminate such as protein and lipid from the culture medium as raw materials by melt spinning, cold drawing, and annealing. They found that as-spun fibers could be cold-drawn at 110°C only immediately after melt spinning. The maximum DR achieved at this drawing temperature was six times. Drawn P(3HB) fibers were stable and no longer changed their thermal and mechanical properties significantly upon storage at room temperature. The properties of P(3HB) fibers depended significantly on the annealing conditions. The strength of fibers annealed without tension was lower than that of unannealed fibers. Annealing under 50 MPa in tensile stress at any temperature examined kept the strength of the fibers close to that of the unannealed fiber. Annealing under 100 MPa increased the strength largely and the strength increased with the increase of the annealing temperature. Annealing at 125°C under 100 MPa in tensile stress produced the fiber with the highest β-form content and the maximum strength. The modulus of the annealed fibers tended to be higher than that of the unannealed fiber, except for the fiber annealed with tension at 150°C. This is due to the crystallization that occurred during the annealing process. In addition, they found that tie molecules between the α-form lamellae in the fiber annealed at high temperature under high tension recrystallized into the β-form. The amorphous tie molecules transformed into orthorhombic crystal during the annealing process without tension.

Vogel et al. [74] prepared P(3HB) fiber by a high-speed melt spinning process using α-cyclodextrin/polymer inclusion complexes as nucleation agents. The results showed that nucleation of P(3HB) within a melt spinning process could be achieved by using α-cyclodextrin/polymer inclusion complexes. And the fibers nucleated with α-cyclodextrin/polymer inclusion complexes exhibited no stick between the single fibers of a multifilament yarn.

Furuhashi et al. [75] prepared P(3HB) fibers by quenching the spinline of P(3HB) below its T_g using ice/methanol bath (−40°C) to keep the amorphous state and drawing it just above T_g in rubbery state to obtain molecular orientation, then conducting further drawing and annealing procedures at higher temperature. The highest tensile strength and tensile modulus of the obtained P(3HB) fibers were 416 MPa and 5.2 GPa, respectively. They found that the β-from crystal was formed not only from the tie chains between α-form lamella, but also from completely free amorphous chains.

Iwata et al. [76] prepared strong P(3HB) fibers from ultra-high-molecular-weight P(3HB) [UHMW-P(3HB)] by cold-drawing and two-step drawing. The amorphous fibers were obtained by quenching the melt-spun fibers of UHMW-PH(3HB) into ice water. The cold-drawing of an amorphous fiber of P(3HB) was possible easily and reproducibly at a temperature below but near to T_g of 4°C in ice water with two sets of rolls. Only chain orientation and slide occurred without crystallization during the cold-drawing. The cold-drawn amorphous fibers were kept at room temperature for several minutes to generate the crystal nucleus, and then two-step drawing was applied with a stretching machine at room temperature. The cold-drawn fibers were drawn at very low stress by more than 1000%, and then an annealing procedure was used to fix the extended polymer chains. The tensile strength and elongation to break as-spun fibers were only 38 MPa and 6%, respectively. After cold-drawing six times in ice water, the tensile strength increased to 121 MPa. The elongation to break was also increased by cold-drawing because the molecular chains aligned in the drawing direction and molecular entanglements decreased during cold-drawing. The tensile strength of two-step-drawn and annealed fibers increased with the ratio of two-step drawing. When the total drawn

ratio reached 60 times (cold-drawn six times and two-step drawn ten times), the tensile strength increased to 1320 MPa. The strong P(3HB) fiber had a core-sheath structure with only a 2_1 helix conformation (α-form) in the sheath region and with both a planar zigzag conformation (β-form) and a 2_1 helix conformation (α-form) in the core region.

Tanaka et al. [77, 78] prepared strong P(3HB-co-3HV) fiber using P(3HB-co-3HV) with low molecular weight. The processing procedures were as follows. Isothermal crystallization of amorphous P(3HB-co-3HV) fiber was held in ice water for a certain period to prevent rapid crystallization and grow small crystal nuclei. One-step drawing after isothermal crystallization was performed with a stretching machine at room temperature, followed by an annealing step at 60°C for 30 min in a hot oven in order to fix the extended polymer chains. One-step-drawn fibers that were isothermally crystallized for 24 h were opaque and their maximum total DR was ca. 10 times with initial length of sample. The tensile strength of as-spun fibers was ca. 30 MPa independent of isothermal crystallization. The tensile strength of a 10 times one-step-drawn fiber without isothermal crystallization was 90 MPa. However, the tensile strength of a 5 times one-step-drawn fiber after isothermal crystallization increased to 710 MPa. Moreover, the tensile strength of a 10 times one-step-drawn fiber after isothermal crystallization further increased to 1065 MPa. This drawing method after isothermal crystallization near T_g was an attractive procedure to obtain strong fibers from P(3HB-co-3HV) with low molecular weight. In addition, one-step-drawn P(3HB-co-3HV) fibers after isothermal crystallization do not have the core-sheath structure observed in cold-drawn and two-step-drawn UHMW-P(3HB) fiber.

Generally speaking, it was thought that the improvement in mechanical properties of P(3HB) and P(3HB-co-3HV) fiber was due not only to the orientation of molecular chains, but also to the generation of a zigzag conformation and network structure, formed by fibrillar and lamellar crystals during processing [79]. Tanaka et al. [77] thought that the presence of the β-form crystals with a planar zigzag conformation was an important factor to generate high-strength P(3HB) and P(3HB-co-3HV) materials. The mechanism for generating the planar zigzag conformation (β-form) in high-strength P(3HB-co-3HV) fibers by different drawing methods including cold-drawing and two-step-drawing and one-step-drawing after isothermal crystallization was illustrated in Figure 6. For UHMW-P(3HB) fiber by cold-drawing and two-step-drawing, the α-form with lamellar crystals was produced by cold-drawing and then the β-form structure with planar zigzag conformation developed during the stretching in the second dimension of the constrained amorphous chains between α-form crystals, as shown in Figure 6(a). The mechanism for the development of β-form crystals for one-step-drawn P(3HB-co-3HV) fibers after isothermal crystallization, as shown in Figure 6(b), was likely to be different from the case of cold-drawn and two-step-drawn fibers. Firstly, many small crystal nuclei grew in the amorphous region by slow crystallization during isothermal crystallization near the T_g. Secondly, the β-form was developed by the stretching of molecular chains in the constrained amorphous region between small crystal nuclei, which acted as cross-linking points. Lastly, the α-form lamellar crystals with various thicknesses were generated from the small crystal nuclei during annealing. It is worth noting that the mechanical properties of commercial-P(3HB) and P(3HB-co-3HV) fibers prepared by one-step-drawing after isothermal crystallization were higher than in the case of UHMW-P(3HB) and P(3HB-co-3HV) fibers [78]. The reason was as follows. In the case of the low-molecular-weight polymer, since the molecular length between the entanglement points of the small crystal nuclei seemed to be almost equivalent to the distance between the entanglement points, it was suitable for generating the extended chains. In the case of UHMW-polymer, because the molecular length between the entanglement points was too long, the molecular chains after stretching could not orient sufficiently [78].

Though the presence of the β-form crystals with a planar zigzag conformations was in general considered to be an important factor to generate high-strength P(3HB) and P(3HB-co-3HV) fiber, Furuhashi et al. thought that the changes in the orientation, number of tie molecules, and other details of the fiber morphology might be more significant in determining the mechanical properties than the relative amounts of α- and β-forms [75].

5. Summary

P(3HB) and P(3HB-co-3HV) are renewable, biodegradable, and thermoplastic with good biocompatibility, which can solve the problems including the shortage of fossil fuels and environmental pollution resulting from nondegradable polymers. In addition, P(3HB) and P(3HB-co-3HV) can be used widely in the medical field. However, some drawbacks for P(3HB) and P(3HB-co-3HV) exist, including brittleness, poor thermal stability, slow crystallization rate, and so on, which restrict the wide application of P(3HB) and P(3HB-co-3HV). It is well known that the properties of polymer are determined by condensed structures of polymer, which are determined by chemical structure and processing fields. Therefore, chemical modification of P(3HB) and P(3HB-co-3HV) should be done to modify the chemical structure of P(3HB) and P(3HB-co-3HV). In addition, the effect of processing fields and chemical structure on the condensed structures and the properties of P(3HB) and P(3HB-co-3HV) should be studied. In this review, it can be seen that the spherulitic morphologies of P(3HB) and P(3HB-co-3HV) can be modified completely by chemical modification of P(3HB) and P(3HB-co-3HV). In addition, the mechanical properties of the different P(3HB) and P(3HB-co-3HV) fibers obtained by different processing conditions are different completely. Therefore, chemical modification of P(3HB) and P(3HB-co-3HV), the relationship between condensed structure and properties of P(3HB) and P(3HB-co-3HV), and chemical

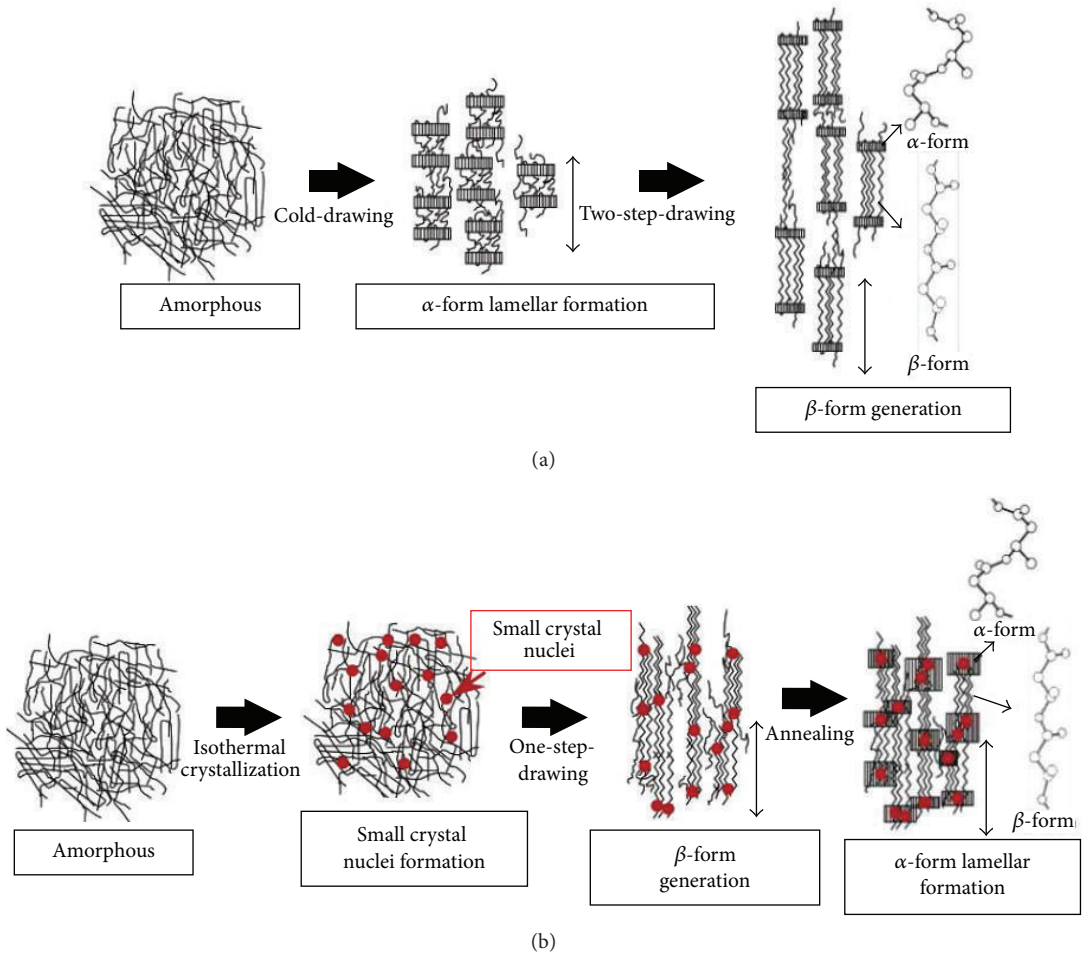

FIGURE 6: Mechanism for generating the planar zigzag conformation (β-form) in high-strength P(3HB-co-3HV) fibers by different drawing methods: (a) cold-drawing and two-step-drawing, and (b) one-step-drawing after isothermal crystallization. The vertical arrows indicate the drawing direction [77].

structure and processing fields have been the focus of this study.

Conflict of Interests

The authors declare that there is no conflict of interests regarding the publication of this paper.

Acknowledgments

This work was supported by the Natural Science Foundation of Jiangsu Province (no. BK20130142), the Open Project Program of Key Laboratory of Advanced Textile Materials and Manufacturing Technology (Zhejiang Sci-Tech University), Ministry of Education (no. 2013004), the Open Project Program of State Key Laboratory for Modification of Chemical Fibers and Polymer Materials, Dong Hua University (no. LK1216), the Public Technology Applied Research Projects of Science Technology Bureau of Shaoxing (no. 2012B70009), the Industrial Support Program (H201313) of Suqian (no. 2012B70009), and the Open Project Program of Key Laboratory of Eco-Textiles, Ministry of Education, Jiangnan University (no. KLET1304).

References

[1] Q. Liu, Y. Chen, and M. Zhu, "Synthesis and characterization of multi-block copolymers containing poly [(3-hydroxybutyrate)-*co*-(3-hydroxyvalerate)] and poly(ethylene glycol)," *Polymer International*, vol. 59, no. 6, pp. 842–850, 2010.

[2] Q.-S. Liu, M.-F. Zhu, W.-H. Wu, and Z.-Y. Qin, "Reducing the formation of six-membered ring ester during thermal degradation of biodegradable PHBV to enhance its thermal stability," *Polymer Degradation and Stability*, vol. 94, no. 1, pp. 18–24, 2009.

[3] I. S. Aldor, *Polyhydroxyalkanoate synthesis in recombinat and environmental microbes [Ph.D. thesis]*, McGill University, Montreal, Canada, 1996.

[4] R. A. J. Verlinden, D. J. Hill, M. A. Kenward, C. D. Williams, and I. Radecka, "Bacterial synthesis of biodegradable polyhydroxyalkanoates," *Journal of Applied Microbiology*, vol. 102, no. 6, pp. 1437–1449, 2007.

[5] M. R. Zakaria, H. Ariffin, N. A. M. Johar et al., "Biosynthesis and characterization of poly(3-hydroxybutyrate-*co*-3-hydroxyvalerate) copolymer from wild-type *Comamonas* sp. EB172," *Polymer Degradation and Stability*, vol. 95, no. 8, pp. 1382–1386, 2010.

[6] D. Z. Bucci, L. B. B. Tavares, and I. Sell, "Biodegradation and physical evaluation of PHB packaging," *Polymer Testing*, vol. 26, no. 7, pp. 908–915, 2007.

[7] J. Mergaert, A. Webb, C. Anderson, A. Wouters, and J. Swings, "Microbial degradation of poly(3-hydroxybutyrate) and poly(3-hydroxybutyrate-*co*-3-hydroxyvalerate) in soils," *Applied and Environmental Microbiology*, vol. 59, no. 10, pp. 3233–3238, 1993.

[8] J. Mergaert, C. Anderson, A. Wouters, and J. Swings, "Microbial degradation of poly(3-hydroxybutyrate) and poly(3-hydroxybutyrate-*co*-3-hydroxyvalerate) in compost," *Journal of Environmental Polymer Degradation*, vol. 2, no. 3, pp. 177–183, 1994.

[9] D. S. Rosa, N. T. Lotto, D. R. Lopes, and C. G. F. Guedes, "The use of roughness for evaluating the biodegradation of poly-β-(hydroxybutyrate) and poly-β-(hydroxybutyrate-*co*-β-valerate)," *Polymer Testing*, vol. 23, no. 1, pp. 3–8, 2004.

[10] D. Akmal, M. N. Azizan, and M. I. A. Majid, "Biodegradation of microbial polyesters P(3HB) and P(3HB-*co*-3HV) under the tropical climate environment," *Polymer Degradation and Stability*, vol. 80, no. 3, pp. 513–518, 2003.

[11] Y.-X. Weng, X.-L. Wang, and Y.-Z. Wang, "Biodegradation behavior of PHAs with different chemical structures under controlled composting conditions," *Polymer Testing*, vol. 30, no. 4, pp. 372–380, 2011.

[12] Z. Li, H. Lin, N. Ishii, G. Chen, and Y. Inoue, "Study of enzymatic degradation of microbial copolyesters consisting of 3-hydroxybutyrate and medium-chain-length 3-hydroxyalkanoates," *Polymer Degradation and Stability*, vol. 92, no. 9, pp. 1708–1714, 2007.

[13] A. N. Boyandin, S. V. Prudnikova, V. A. Karpov et al., "Microbial degradation of polyhydroxyalkanoates in tropical soils," *International Biodeterioration & Biodegradation*, vol. 83, pp. 77–84, 2013.

[14] G. Cheng, Z. Cai, and L. Wang, "Biocompatibility and biodegradation of poly(hydroxybutyrate)/poly(ethylene glycol) blend films," *Journal of Materials Science: Materials in Medicine*, vol. 14, no. 12, pp. 1073–1078, 2003.

[15] G. G. Choi, H. W. Kim, Y. B. Kim, and Y. H. Rhee, "Biocompatibility of poly(3-hydroxybutyrate-*co*-3-hydroxyvalerate) copolyesters produced by *Alcaligenes* sp. MT-16," *Biotechnology and Bioprocess Engineering*, vol. 10, no. 6, pp. 540–545, 2005.

[16] Z. Cai, G. Yang, and J. Kim, "Biocompatible nanocomposites prepared by impregnating bacterial cellulose nanofibrils into poly(3-hydroxybutyrate)," *Current Applied Physics*, vol. 11, no. 2, pp. 247–249, 2011.

[17] R. W. Lenz and R. H. Marchessault, "Bacterial polyesters: biosynthesis, biodegradable plastics and biotechnology," *Biomacromolecules*, vol. 6, no. 1, pp. 1–8, 2005.

[18] Q. Liu, B. Deng, C.-H. Tung, M. Zhu, and T.-W. Shyr, "Nonisothermal crystallization kinetics of poly(ε-caprolactone) blocks in double crystalline triblock copolymers containing poly(3-hydroxybutyrate-*co*-3-hydroxyvalerate) and poly(ε-caprolactone) units," *Journal of Polymer Science B: Polymer Physics*, vol. 48, no. 21, pp. 2288–2295, 2010.

[19] Q. Liu, T.-W. Shyr, C.-H. Tung, B. Deng, and M. Zhu, "Block copolymers containing poly (3-hydroxybutyrate-*co*-3-hydroxyvalerate) and poly (ε-caprolactone) units: synthesis, characterization and thermal degradation," *Fibers and Polymers*, vol. 12, no. 7, pp. 848–856, 2011.

[20] J. L. Ienczak, W. Schmidell, and G. M. F. de Aragão, "High-cell-density culture strategies for polyhydroxyalkanoate production: a review," *Journal of Industrial Microbiology and Biotechnology*, vol. 40, no. 3-4, pp. 275–286, 2013.

[21] D. K. Y. Solaiman, R. D. Ashby, T. A. Foglia, and W. N. Marmer, "Conversion of agricultural feedstock and coproducts into poly(hydroxyalkanoates)," *Applied Microbiology and Biotechnology*, vol. 71, no. 6, pp. 783–789, 2006.

[22] J. Choi and S. Y. Lee, "Factors affecting the economics of polyhydroxyalkanoate production by bacterial fermentation," *Applied Microbiology and Biotechnology*, vol. 51, no. 1, pp. 13–21, 1999.

[23] N. Jacquel, C. Lo, Y. Wei, H. Wu, and S. S. Wang, "Isolation and purification of bacterial poly(3-hydroxyalkanoates)," *Biochemical Engineering Journal*, vol. 39, no. 1, pp. 15–27, 2008.

[24] A. Ishizaki, K. Tanaka, and N. Taga, "Microbial production of poly-D-3-hydroxybutyrate from CO_2," *Applied Microbiology and Biotechnology*, vol. 57, no. 1-2, pp. 6–12, 2001.

[25] T. M. Keenan, J. P. Nakas, and S. W. Tanenbaum, "Polyhydroxyalkanoate copolymers from forest biomass," *Journal of Industrial Microbiology and Biotechnology*, vol. 33, no. 7, pp. 616–626, 2006.

[26] G. Braunegg, G. Lefebvre, and K. F. Genser, "Polyhydroxyalkanoates, biopolyesters from renewable resources: physiological and engineering aspects," *Journal of Biotechnology*, vol. 65, no. 2-3, pp. 127–161, 1998.

[27] S. Y. Lee and J. Choi, "Production and degradation of polyhydroxyalkanoates in waste environment," *Waste Management*, vol. 19, no. 2, pp. 133–139, 1999.

[28] S. Y. Lee, J. Choi, and H. H. Wong, "Recent advances in polyhydroxyalkanoate production by bacterial fermentation: mini-review," *International Journal of Biological Macromolecules*, vol. 25, no. 1-3, pp. 31–36, 1999.

[29] L. S. Serafim, P. C. Lemos, M. G. E. Albuquerque, and M. A. M. Reis, "Strategies for PHA production by mixed cultures and renewable waste materials," *Applied Microbiology and Biotechnology*, vol. 81, no. 4, pp. 615–628, 2008.

[30] K. Sudesh, H. Abe, and Y. Doi, "Synthesis, structure and properties of polyhydroxyalkanoates: biological polyesters," *Progress in Polymer Science*, vol. 25, no. 10, pp. 1503–1555, 2000.

[31] R. Li, H. Zhang, and Q. Qi, "The production of polyhydroxyalkanoates in recombinant *Escherichia coli*," *Bioresource Technology*, vol. 98, no. 12, pp. 2313–2320, 2007.

[32] D. Y. Kim and Y. H. Rhee, "Biodegradation of microbial and synthetic polyesters by fungi," *Applied Microbiology and Biotechnology*, vol. 61, no. 4, pp. 300–308, 2003.

[33] J. Mas-Castellà, J. Urmeneta, R. Lafuente, A. Navarrete, and R. Guerrero, "Biodegradation of poly-β-hydroxyalkanoates in anaerobic sediments," *International Biodeterioration and Biodegradation*, vol. 35, no. 1–3, pp. 155–174, 1995.

[34] Y. Tokiwa and B. P. Calabia, "Degradation of microbial polyesters," *Biotechnology Letters*, vol. 26, no. 15, pp. 1181–1189, 2004.

[35] D. Jendrossek, "Microbial degradation of polyesters: a review on extracellular poly(hydroxy alkanoic acid) depolymerases," *Polymer Degradation and Stability*, vol. 59, no. 1–3, pp. 317–325, 1998.

[36] B. Laycock, P. Halley, S. Pratt, A. Werker, and P. Lant, "The chemomechanical properties of microbial polyhydroxyalkanoates," *Progress in Polymer Science*, vol. 38, no. 3-4, pp. 536–583, 2013.

[37] C. Ha and W. Cho, "Miscibility, properties, and biodegradability of microbial polyester containing blends," *Progress in Polymer Science*, vol. 27, no. 4, pp. 759–809, 2002.

[38] M. Avella, E. Martuscelli, and M. Raimo, "Properties of blends and composites based on poly(3-hydroxy)butyrate (PHB) and poly(3-hydroxybutyrate-hydroxyvalerate) (PHBV) copolymers," *Journal of Materials Science*, vol. 35, no. 3, pp. 523–545, 2000.

[39] N. Yoshie and Y. Inoue, "Cocrystallization and phase segregation in blends of two bacterial polyesters," *Macromolecular Symposia*, vol. 224, pp. 59–70, 2005.

[40] C. J. Brigham and A. J. Sinskey, "Application of polyhydroxyalkanoates in the medical industry," *International Journal of Biotechnology for Wellness Industries*, vol. 1, pp. 53–60, 2012.

[41] T. Freier, "Biopolyesters in tissue engineering applications," *Advances in Polymer Science*, vol. 203, no. 1, pp. 1–61, 2006.

[42] S. K. Misra, S. P. Valappil, I. Roy, and A. R. Boccaccini, "Polyhydroxyalkanoate (PHA)/inorganic phase composites for tissue engineering applications," *Biomacromolecules*, vol. 7, no. 8, pp. 2249–2258, 2006.

[43] G. Chen and Q. Wu, "The application of polyhydroxyalkanoates as tissue engineering materials," *Biomaterials*, vol. 26, no. 33, pp. 6565–6578, 2005.

[44] O. Miguel and J. J. Iruin, "Evaluation of the transport properties of poly(3-hydroxybutyrate) and its 3-hydroxyvalerate copolymers for packaging applications," *Macromolecular Symposia*, vol. 144, no. 1, pp. 427–438, 1999.

[45] L. Wang, J. Du, D. Cao, and Y. Wang, "Recent advances and the application of poly(3-hydroxybutyrate-*co*-3-hydroxyvalerate) as tissue engineering materials," *Journal of Macromolecular Science A: Pure and Applied Chemistry*, vol. 50, no. 8, pp. 885–893, 2013.

[46] M. Kunioka, A. Tamaki, and Y. Doi, "Crystalline and thermal properties of bacterial copolyesters: poly(3-hydroxybutyrate-*co*-3-hydroxyvalerate) and poly(3-hydroxybutyrate-*co*-4-hydroxybutyrate)," *Macromolecules*, vol. 22, no. 2, pp. 694–697, 1989.

[47] M. Scandola, G. Ceccorulli, M. Pizzoli, and M. Gazzano, "Study of the crystal phase and crystallization rate of bacterial poly(3-hydroxybutyrate-*co*-3-hydroxyvalerate)," *Macromolecules*, vol. 25, no. 5, pp. 1405–1410, 1992.

[48] S. Bloembergen, D. A. Holden, G. K. Hamer, T. L. Bluhm, and R. H. Marchessault, "Studies of composition and crystallinity of bacterial poly(β-hydroxybutyrate-*co*-β-hydroxyvalerate)," *Macromolecules*, vol. 19, no. 11, pp. 2865–2871, 1986.

[49] T. L. Bluhm, G. K. Hamer, R. H. Marchessault, C. A. Fyfe, and R. P. Veregin, "Isodimorphism in bacterial poly(β-hydroxybutyrate-*co*-β-hydroxyvalerate)," *Macromolecules*, vol. 19, no. 11, pp. 2871–2876, 1986.

[50] P. A. Barker, P. J. Barham, and J. Martinez-Salazar, "Effect of crystallization temperature on the cocrystallization of hydroxybutyrate/ hydroxyvalerate copolymers," *Polymer*, vol. 38, no. 4, pp. 913–919, 1997.

[51] N. Yoshie, M. Saito, and Y. Inoue, "Structural transition of lamella crystals in a isomorphous copolymer, poly(3-hydroxybutyrate-*co*-3-hydroxyvalerate)," *Macromolecules*, vol. 34, no. 26, pp. 8953–8960, 2001.

[52] H. Sato, Y. Ando, H. Mitomo, and Y. Ozaki, "Infrared spectroscopy and X-ray diffraction studies of thermal behavior and lamella structures of poly(3-hydroxybutyrate-*co*-3-hydroxyvalerate) (P(HB-co-HV)) with PHB-Type crystal structure and PHV-Type crystal structure," *Macromolecules*, vol. 44, no. 8, pp. 2829–2837, 2011.

[53] G. Ding and J. Liu, "Morphological varieties and kinetic behaviors of poly(3-hydroxybutyrate) (PHB) spherulites crystallized isothermally from thin melt film," *Colloid and Polymer Science*, vol. 291, no. 6, pp. 1547–1554, 2013.

[54] Y. Jiang, J.-J. Zhou, L. Li et al., "Surface properties of poly(3-hydroxybutyrate-*co*-3-hydroxyvalerate) banded spherulites studied by atomic force microscopy and time-of-flight secondary ion mass spectrometry," *Langmuir*, vol. 19, no. 18, pp. 7417–7422, 2003.

[55] Z. Wang, Y. Li, J. Yang et al., "Twisting of lamellar crystals in poly(3-hydroxybutyrate-*co*-3-hydroxyvalerate) ring-banded spherulites," *Macromolecules*, vol. 43, no. 10, pp. 4441–4444, 2010.

[56] Q. Liu, M. Zhu, B. Deng, C. H. Tung, and T. W. Shyr, "Evolution of concentric spherulites in crystalline-crystalline poly(3-hydroxybutyrate-*co*-3-hydroxyvalerate)-b-poly(ethylene glycol) copolymers," *European Polymer Journal*, vol. 49, no. 12, pp. 3937–3946, 2013.

[57] Q. Liu, M. Zhu, C.-H. Tung, T.-W. Shyr, and B. Deng, "Peculiar spherulitic morphologies and melting behavior of block copolymer containing poly(3-hydroxybutyrate-*co*-3-hydroxyvalerate) and poly(ε-caprolactone) units," *Macromolecular Research*, vol. 19, no. 12, pp. 1220–1223, 2011.

[58] H. Sato, R. Murakami, A. Padermshoke et al., "Infrared spectroscopy studies of CH$\cdots$O hydrogen bondings and thermal behavior of biodegradable poly(hydroxyalkanoate)," *Macromolecules*, vol. 37, no. 19, pp. 7203–7213, 2004.

[59] H. Sato, J. Dybal, R. Murakami, I. Noda, and Y. Ozaki, "Infrared and Raman spectroscopy and quantum chemistry calculation studies of C-H$\cdots$O hydrogen bondings and thermal behavior of biodegradable polyhydroxyalkanoate," *Journal of Molecular Structure*, vol. 744–747, pp. 35–46, 2005.

[60] H. Sato, K. Mori, R. Murakami et al., "Crystal and lamella structure and C-H$\cdots$O=C hydrogen bonding of poly(3-hydroxyalkanoate) studied by X-ray diffraction and infrared spectroscopy," *Macromolecules*, vol. 39, no. 4, pp. 1525–1531, 2006.

[61] Y. Hu, J. Zhang, H. Sato, Y. Futami, I. Noda, and Y. Ozaki, "C-H$\cdots$O=C hydrogen bonding and isothermal crystallization kinetics of poly(3-hydroxybutyrate) investigated by near-infrared spectroscopy," *Macromolecules*, vol. 39, no. 11, pp. 3841–3847, 2006.

[62] Q. Liu, T.-W. Shyr, C.-H. Tung et al., "Particular thermal properties of poly(3-hydroxybutyrateco-3-hydroxyvalerate) oligomers," *Journal of Polymer Research*, vol. 19, no. 1, article 9756, 2012.

[63] W. Kai, Y. He, and Y. Inoue, "Fast crystallization of poly(3-hydroxybutyrate) and poly(3-hydroxybutyrate-*co*-3-hydroxyvalerate) with talc and boron nitride as nucleating agents," *Polymer International*, vol. 54, no. 5, pp. 780–789, 2005.

[64] J. Li, M. F. Lai, and J. J. Liu, "Effect of poly(propylene carbonate) on the crystallization and melting behavior of poly(β-hydroxybutyrate-*co*-β-hydroxyvalerate)," *Journal of Applied Polymer Science*, vol. 92, no. 4, pp. 2514–2521, 2004.

[65] W. J. Liu, H. L. Yang, Z. Wang, L. S. Dong, and J. J. Liu, "Effect of nucleating agents on the crystallization of poly(3-hydroxybutyrate-*co*-3-hydroxyvalerate)," *Journal of Applied Polymer Science*, vol. 86, no. 9, pp. 2145–2152, 2002.

[66] M. L. D. Lorenzo and M. C. Righetti, "Evolution of crystal and amorphous fractions of poly[(R)-3-hydroxybutyrate] upon storage," *Journal of Thermal Analysis and Calorimetry*, vol. 112, no. 3, pp. 1439–1446, 2013.

[67] M. L. D. Lorenzo and M. C. Righetti, "Effect of thermal history on the evolution of crystal and amorphous fractions of poly[(R)-3-hydroxybutyrate] upon storage at ambient temperature," *European Polymer Journal*, vol. 49, no. 2, pp. 510–517, 2013.

[68] M. Zinn, B. Witholt, and T. Egli, "Occurrence, synthesis and medical application of bacterial polyhydroxyalkanoate," *Advanced Drug Delivery Reviews*, vol. 53, no. 1, pp. 5–21, 2001.

[69] A. Shikanov, N. Kumar, and A. J. Domb, "Biodegradable polymers: an update," *Israel Journal of Chemistry*, vol. 45, no. 4, pp. 393–399, 2005.

[70] S. A. Gordeyev and Y. P. Nekrasov, "Processing and mechanical properties of oriented poly(β-hydroxybutyrate) fibers," *Journal of Materials Science Letters*, vol. 18, no. 20, pp. 1691–1692, 1999.

[71] S. A. Gordeyev, Y. P. Nekrasov, and S. J. Shilton, "Processing of gel-spun poly(β-hydroxybutyrate) fibers," *Journal of Applied Polymer Science*, vol. 81, no. 9, pp. 2260–2264, 2001.

[72] G. Schmack, D. Jehnichen, R. Vogel, and B. Tändler, "Biodegradable fibers of poly(3-hydroxybutyrate) produced by high-speed melt spinning and spin drawing," *Journal of Polymer Science B: Polymer Physics*, vol. 38, no. 21, pp. 2841–2850, 2000.

[73] H. Yamane, K. Terao, S. Hiki, and Y. Kimura, "Mechanical properties and higher order structure of bacterial homo poly(3-hydroxybutyrate) melt spun fibers," *Polymer*, vol. 42, no. 7, pp. 3241–3248, 2001.

[74] R. Vogel, B. Tändler, L. Häussler, D. Jehnichen, and H. Brünig, "Melt spinning of poly(3-hydroxybutyrate) fibers for tissue engineering using α-cyclodextrin/polymer inclusion complexes as the nucleation agent," *Macromolecular Bioscience*, vol. 6, no. 9, pp. 730–736, 2006.

[75] Y. Furuhashi, Y. Imamura, Y. Jikihara, and H. Yamane, "Higher order structures and mechanical properties of bacterial homo poly(3-hydroxybutyrate) fibers prepared by cold-drawing and annealing processes," *Polymer*, vol. 45, no. 16, pp. 5703–5712, 2004.

[76] T. Iwata, Y. Aoyagi, M. Fujita et al., "Processing of a strong biodegradable poly[(R)-3-hydroxybutyrate] fiber and a new fiber structure revealed by micro-beam x-ray diffraction with synchrotron radiation," *Macromolecular Rapid Communications*, vol. 25, no. 11, pp. 1100–1104, 2004.

[77] T. Tanaka, M. Fujita, A. Takeuchi et al., "Formation of highly ordered structure in poly[(R)-3-hydroxybutyrate-*co*-(R)-3-hydroxyvalerate] high-strength fibers," *Macromolecules*, vol. 39, no. 8, pp. 2940–2946, 2006.

[78] T. Tanaka, T. Yabe, S. Teramachi, and T. Iwata, "Mechanical properties and enzymatic degradation of poly[(R)-3-hydroxybutyrate] fibers stretched after isothermal crystallization near T_g," *Polymer Degradation and Stability*, vol. 92, no. 6, pp. 1016–1024, 2007.

[79] T. Iwata, "Strong fibers and films of microbial polyesters," *Macromolecular Bioscience*, vol. 5, no. 8, pp. 689–701, 2005.